PHYSICAL REVIEW D **78,** 093001 (2008)

Higgs triplets, decoupling, and precision measurements

Mu-Chun Chen,[1,*] Sally Dawson,[2,+] and C. B. Jackson[3,‡]

[1]*Department of Physics and Astronomy, University of California, Irvine, California 92697, USA*

[2]*Department of Physics, Brookhaven National Laboratory, Upton, New York 11973, USA*

[3]*HEP Division, Argonne National Laboratory, 9700 Cass Avenue Argonne, Illinois 60439, USA*

(Received 24 September 2008; published 4 November 2008)

Electroweak precision data has been extensively used to constrain models containing physics beyond that of the standard model. When the model contains Higgs scalars in representations other than $SU(2)$ singlets or doublets, and hence $\rho \neq 1$ at tree level, a correct renormalization scheme requires more inputs than the three needed for the standard model. We discuss the connection between the renormalization of models with Higgs triplets and the decoupling properties of the models as the mass scale for the scalar triplet field becomes much larger than the electroweak scale. The requirements of perturbativity of the couplings and agreement with electroweak data place strong restrictions on models with Higgs triplets. Our results have important implications for Little Higgs type models and other models with $\rho \neq 1$ at tree level.

DOI: 10.1103/PhysRevD.78.093001 PACS numbers: 12.15.Lk

I. INTRODUCTION

The standard model (SM) of electroweak physics is remarkably successful at explaining experimental data. From a theoretical standpoint, however, the theory has many failings. Attempts to address these perceived inadequacies have led to the construction of models which reduce to the standard nodel at energy scales below about 1 TeV, but which differ at higher energies. Models with physics beyond that of the standard model, however, are severely constrained by precision electroweak data [1,2]. If the mass scale of the new physics is near the TeV scale, it is often possible to learn about the parameters of the model by performing global fits to precision measurements. The simplest example is the prediction of the W boson mass, M_W. In thestandard model, M_W can be predicted in terms of other parameters of the theory and requiring agreement with the measured W mass therefore restricts the possibilities for new TeV scale physics.

In this paper, we introduce a Higgs triplet at the electroweak scale and consider the effect on M_W [3–6]. We are motivated by Little Higgs models, which include a scalar triplet as a necessary ingredient, although our results are very general [7–14]. In a model with Higgs particles in representations other than $SU(2)$ doublets and singlets, there are more parameters in the gauge/Higgs sector than in the standard model. The SM tree-level relation, $\rho = M_W^2/(M_Z^2 c_\theta^2) = 1$, no longer holds and when the theory is renormalized an extra input parameter is required [3–6,14–18]. We discuss two possible renormalization schemes for the triplet model: one where the extra parameter is chosen to be a low-energy observable [3–5], and one where the extra parameter is taken to be the running vacuum expectation value (VEV) of the triplet scalar [19,20]. Models with $\rho = M_W^2/(M_Z^2 c_\theta^2) \neq 1$ can be consistent with experimental data with the inclusion of certain types of new physics [21,22], of which a Higgs triplet is a specific example.

In Sec. II we describe a model which contains a real Higgs triplet in addition to the Higgs doublet of the standard model. This example is a simplified version of the Higgs sector in Little Higgs models and is the simplest example of a model with $\rho \neq 1$ at tree level. In Sec. III, we discuss the restrictions on models with scalar triplets at the electroweak scale from requiring perturbativity of the parameters of the scalar potential. We turn in Sec. IV to a discussion of the renormalization prescription and the role of the triplet vacuum expectation value. The role of the scalar particles is emphasized in obtaining predictions for M_W in the triplet model [23]. Whereas in the SM, the Higgs scalar contributes logarithmically to the prediction for M_W, in the triplet model there are contributions which grow with the scalar masses-squared [24–27]. We close in Sec. V with a discussion of the decoupling of Higgs triplet effects for large mass scales or alternatively in the limit that the triplet VEV goes to zero and we draw some general conclusions about the renormalization scheme dependence in models with $\rho \neq 1$ at tree limit.

II. THE MODEL

We consider a model with a real Higgs doublet, H, and a real isospin $Y = 0$ triplet, Φ. We assume that the scalar potential is such that the neutral components of both the doublet and the triplet receive VEVs, breaking the electro-

*muchunc@uci.edu
+dawson@bnl.gov
‡jackson@hep.anl.gov

weak symmetry. The scalars are conventionally written as

$$H = \begin{pmatrix} \phi^+ \\ \frac{1}{\sqrt{2}}(v + h^0 + i\chi^0) \end{pmatrix}, \qquad \Phi = \begin{pmatrix} \eta^+ \\ v' + \eta^0 \\ -\eta^- \end{pmatrix}. \quad (1)$$

The kinetic part of the Lagrangian is

$$L = |D_\mu H|^2 + \frac{1}{2}|D_\mu \Phi|^2, \quad (2)$$

where,

$$D_\mu H = \left(\partial_\mu + i\frac{g}{2}\sigma^a W^a + i\frac{g'}{2} Y B_\mu\right) H$$
$$D_\mu \Phi = (\partial_\mu + i g t_a W^a)\Phi, \quad (3)$$

σ^a ($a = 1, 2, 3$) are the Pauli matrices, and

$$t_1 = \frac{1}{\sqrt{2}}\begin{pmatrix} 0 & 1 & 0 \\ 1 & 0 & 1 \\ 0 & 1 & 0 \end{pmatrix}, \qquad t_2 = \frac{1}{\sqrt{2}}\begin{pmatrix} 0 & -i & 0 \\ i & 0 & -i \\ 0 & i & 0 \end{pmatrix},$$
$$t_3 = \begin{pmatrix} 1 & 0 & 0 \\ 0 & 0 & 0 \\ 0 & 0 & -1 \end{pmatrix}. \quad (4)$$

Spontaneous symmetry breaking generates masses for the W and Z bosons,

$$M_W^2 = \frac{g^2}{4}(v^2 + 4v'^2) \qquad M_Z^2 = \frac{g^2}{4c_\theta^2} v^2, \quad (5)$$

where $c_\theta \equiv \cos\theta = g/\sqrt{(g')^2 + (g)^2}$ and $\sin\theta \equiv s_\theta$. At tree level, all definitions of c_θ are equivalent and the VEVs are related to the SM VEV by $v_{\rm SM}^2 = (246\ \text{GeV})^2 = v^2 + 4v'^2$.

The model violates custodial symmetry at tree level,

$$\rho = \frac{M_W^2}{M_Z^2 c_\theta^2} = 1 + 4\frac{v'^2}{v^2}. \quad (6)$$

Since experimentally $\rho \sim 1$, v' will be restricted to be small. Neglecting scalar loops, Refs. [1,2] found $v' < 12$ GeV.

The most general $SU(2) \times U(1)$ scalar potential with a Higgs doublet and a real scalar triplet is given by

$$V = \mu_1^2 |H|^2 + \frac{\mu_2^2}{2}|\Phi|^2 + \lambda_1 |H|^4 + \frac{\lambda_2}{4}|\Phi|^4$$
$$+ \frac{\lambda_3}{2}|H|^2|\Phi|^2 + \lambda_4 H^\dagger \sigma^a H \Phi_a. \quad (7)$$

We note that the coefficient λ_4 has dimensions of mass, which implies that its effects may be important even for large mass scales since the decoupling theorem is not applicable to interactions which are proportional to mass [3,28,29].

After spontaneous symmetry breaking, there are two physical neutral eigenstates, H^0, K^0,

$$\begin{pmatrix} H^0 \\ K^0 \end{pmatrix} = \begin{pmatrix} c_\gamma & s_\gamma \\ -s_\gamma & c_\gamma \end{pmatrix}\begin{pmatrix} h^0 \\ \eta^0 \end{pmatrix}. \quad (8)$$

The physical charged eigenstates are $H^\pm$ and the charged Goldstone bosons which become the longitudinal components of the $W^\pm$ bosons are $G^\pm$,

$$\begin{pmatrix} G^+ \\ H^+ \end{pmatrix} = \begin{pmatrix} c_\delta & s_\delta \\ -s_\delta & c_\delta \end{pmatrix}\begin{pmatrix} \phi^+ \\ \eta^+ \end{pmatrix}, \quad (9)$$

where $\tan\delta = 2v'/v$.

Minimizing the potential gives the tree-level relations:

$$0 = \mu_1^2 + \lambda_1 v^2 + \frac{\lambda_3}{2}v'^2 - \lambda_4 v' \quad (10)$$

$$0 = v'\left(\mu_2^2 + \lambda_2 v'^2 + \lambda_3\frac{v^2}{2}\right) - \lambda_4\frac{v^2}{2}. \quad (11)$$

For $v' = 0$, the only consistent solution to the minimization of the potential has $M_{K^0} = M_{H^+}$ and $\lambda_4 = \sin\delta = \sin\gamma = 0$. In this limit the custodial symmetry is restored and $\rho = 1$ at tree level.

We assume that $v' \neq 0$ and $\gamma \neq 0$. Utilizing Eqs. (10) and (11), the scalar mass eigenstates are [30]

$$M_{H^+}^2 = \frac{\lambda_4 v}{c_\delta s_\delta} \qquad M_{H^0}^2 = 2\lambda_1 v^2 + \tan\gamma(\lambda_3 v v' - \lambda_4 v)$$
$$M_{K^0}^2 = 2\lambda_1 v^2 - \cot\gamma(\lambda_3 v v' - \lambda_4 v). \quad (12)$$

We take as our six input parameters in the scalar sector, M_{H^+}, M_{H^0}, M_{K^0}, γ, δ, v. Inverting Eq. (12),

$$\lambda_1 = \frac{1}{2v^2}(c_\gamma^2 M_{H^0}^2 + s_\gamma^2 M_{K^0}^2)$$
$$\lambda_2 = \frac{2}{v^2}\cot^2\delta[s_\gamma^2 M_{H^0}^2 + c_\gamma^2 M_{K^0}^2 - c_\delta^2 M_{H^+}^2]$$
$$\lambda_3 = \frac{1}{v^2\tan\delta}[(M_{H^0}^2 - M_{K^0}^2)\sin(2\gamma) + M_{H^+}^2\sin(2\delta)]$$
$$\lambda_4 = c_\delta s_\delta\frac{M_{H^+}^2}{v}$$
$$\mu_1^2 = -\frac{M_{H^0}^2}{2}\left(c_\gamma^2 + \frac{s_\gamma c_\gamma}{2}\tan\delta\right)$$
$$- \frac{M_{K^0}^2}{2}\left(s_\gamma^2 - \frac{s_\gamma c_\gamma}{2}\tan\delta\right) + \frac{M_{H^+}^2}{4}s_\delta^2$$
$$\mu_2^2 = \frac{c_\delta^2}{2}M_{H^+}^2 - \frac{M_{H^0}^2}{2}(s_\gamma^2 + \sin(2\gamma)\cot\delta)$$
$$- \frac{M_{K^0}^2}{2}(c_\gamma^2 - \sin(2\gamma)\cot\delta). \quad (13)$$

III. PERTURBATIVITY OF THE SCALAR COUPLINGS

A priori, the input parameters, M_{H^+}, M_{H^0}, M_{K^0}, γ, δ, v, are arbitrary. The requirement that the tree-level contribu-

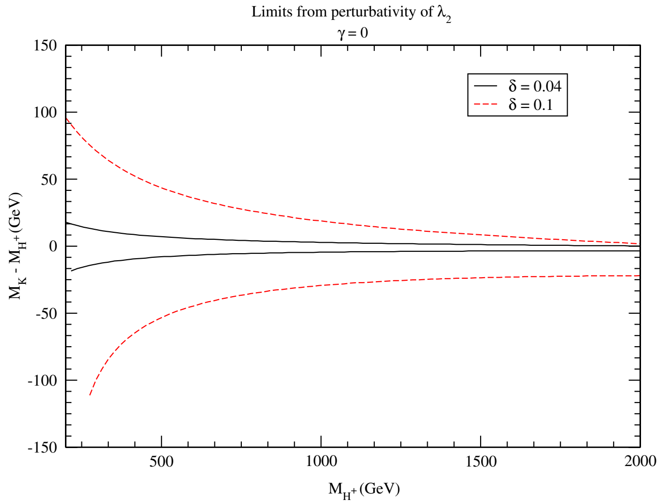

FIG. 1 (color online). Restriction on the mass difference, $M_{K^0} - M_{H^+}$ from the requirement that the scalar coupling, λ_2, be perturbative, $\lambda_2 \lesssim (4\pi)^2$. For $\gamma = 0$, there is no dependence on M_{H^0}.

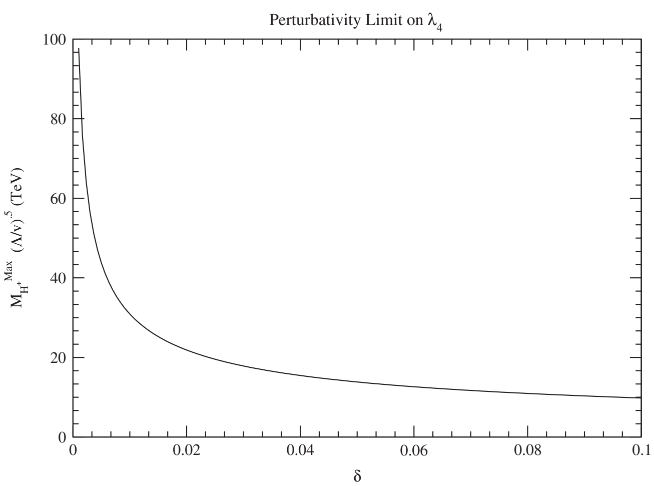

FIG. 2. Restriction on the charged scalar mass from the requirement that the scalar coupling, λ_4, be perturbative, $\frac{\lambda_4}{\Lambda} \lesssim (4\pi)^2$.

tions to the scalar self-interactions be larger than the one-loop contributions can be loosely interpreted as the restriction $\lambda_{1,2,3} < (4\pi)^2$, and $\frac{\lambda_4}{\Lambda} < (4\pi)^2$ (the scale Λ is arbitrary).

From Eq. (13), approximate bounds on the scalar masses can be derived.[1] The most restrictive bound on M_{H^0} is found from $\lambda_1 \lesssim (4\pi)^2$ for $c_\gamma \sim 1$,

$$M_{H^0} \lesssim 4.4 \text{ TeV}. \tag{14}$$

An interesting limit on the mass difference between the charged scalar, H^+, and the heavier of the neutral scalars, K^0, comes from Eq. (13) and the requirement that $\lambda_2 \lesssim (4\pi)^2$. This restriction is illustrated in Fig. 1. As the mass of M_{H^+} becomes large, perturbativity requires that the mass difference between M_{K^0} and M_H^+ be small, regardless of the mixing parameters. Similarly, assuming a scale $\Lambda \sim v$, the perturbativity limits on M_{H^+} from λ_4 are shown in Fig. 2. These results are in agreement with those found in Refs. [28,30].

IV. RENORMALIZATION

A. Standard model

In this section, we discuss the differences between renormalization in the SM and in a model with a scalar triplet. We begin with a brief overview of standard model renormalization in order to set the framework [31–34]. The electroweak sector of the SM has four fundamental parameters, the $SU(2)_L \times U(1)_Y$ gauge coupling constants, g and g', the vacuum expectation value of the neutral component of the Higgs doublet, v, and the physical Higgs boson mass, along with the fermion masses. Once these parameters are fixed, all other physical quantities in the gauge sector can be derived. The usual choice of input parameters is the muon decay constant, G_μ, the Z-boson mass, M_Z, the fine structure constant, α, and the unknown Higgs boson mass, $M_{h,\text{SM}}$. Experimentally, the measured values for these input parameters are [35]

$$G_\mu = 1.16637(1) \times 10^{-5} \text{ GeV}^{-2} \tag{15}$$

$$M_Z = 91.1876(21) \text{ GeV} \tag{16}$$

$$\alpha^{-1} = 137.035999679(94). \tag{17}$$

Tree-level objects are denoted with a subscript 0 and satisfy the relationship,

$$M_{W0}^2 = \frac{\pi\alpha_0}{\sqrt{2}G_{\mu 0}s_{\theta 0}^2}, \tag{18}$$

and the SM satisfies $\rho_0 = 1$ at tree level,

$$\rho_0 \equiv \frac{M_{W0}^2}{M_{Z0}^2 c_{\theta 0}^2} = 1. \tag{19}$$

[1] Ref. [30] derived the renormalization group improved bounds on the scalar masses. For our purposes the tree-level bounds are sufficient.

The one-loop renormalized quantitites are defined[2]:

$$\begin{aligned} M_{V0}^2 &\equiv M_V^2\left(1+\frac{\delta M_V^2}{M_V^2}\right) = M_V^2(1+\Pi_{VV}(M_V^2)) \\ G_{\mu 0} &\equiv G_\mu\left(1+\frac{\delta G_\mu}{G_\mu}\right) = G_\mu\left(1-\frac{\Pi_{WW}(0)}{M_W^2}\right) \\ s_{\theta 0}^2 &= s_\theta^2\left(1+\frac{\delta s_\theta^2}{s_\theta^2}\right) \\ \alpha_0 &= \alpha\left(1+\frac{\delta\alpha}{\alpha}\right) = \alpha\left(1+\Pi'_{\gamma\gamma}(0)+2\frac{s_\theta}{c_\theta}\frac{\Pi_{\gamma Z}(0)}{M_Z^2}\right), \end{aligned} \tag{20}$$

where $\Pi'_{\gamma\gamma}(0) = (d\Pi_{\gamma\gamma}(p^2)/dp^2)|_{p^2=0} \sim \frac{\Pi_{\gamma\gamma}(M_Z^2)}{M_Z^2}$. The box and vertex corrections are small, and we neglect their finite contributions (although it is necessary to include the poles in order to achieve a finite result).

The W-boson mass is predicted at one-loop,

$$M_W^2 = \frac{\pi\alpha}{\sqrt{2}G_\mu s_\theta^2}[1+\Delta r_{\rm SM}], \tag{21}$$

where $\Delta r_{\rm SM}$ summarizes the radiative corrections,

$$\begin{aligned} \Delta r_{\rm SM} &= -\frac{\delta G_\mu}{G_\mu} - \frac{\delta M_W^2}{M_W^2} + \frac{\delta\alpha}{\alpha} - \frac{\delta s_\theta^2}{s_\theta^2} \\ &= \frac{\Pi_{WW,\rm SM}(0) - \Pi_{WW,\rm SM}(M_W^2)}{M_W^2} + \Pi'_{\gamma\gamma,\rm SM}(0) \\ &\quad + 2\frac{s_\theta}{c_\theta}\frac{\Pi_{\gamma Z,\rm SM}(0)}{M_Z^2} - \frac{\delta s_\theta^2}{s_\theta^2}. \end{aligned} \tag{22}$$

We use $s_\theta \equiv \sin\theta$, $c_\theta \equiv \cos\theta$ to denote a generic definition of the weak mixing angle. At tree level all definitions are equal and we consider three possible definitions of the weak mixing angle, which differ only at one-loop and are useful for comparing with the predictions of the triplet model in the next section and for understanding the renormalization scheme dependence of the triplet model predictions. For clarity, we review these definitions briefly [36].

1. *On-shell definition of* $\sin\theta_W$

In the on-shell scheme, the weak mixing angle, s_W, is not a free parameter, but is derived from

$$\rho \equiv \frac{M_W^2}{M_Z^2 c_W^2}. \tag{23}$$

The counter term for s_W^2 can be derived from Eq. (23):

$$\begin{aligned} \frac{\delta s_W^2}{s_W^2} &= \frac{c_W^2}{s_W^2}\left[\frac{\delta M_Z^2}{M_Z^2} - \frac{\delta M_W^2}{M_W^2}\right] \\ &= \frac{c_W^2}{s_W^2}\left[\frac{\Pi_{ZZ,\rm SM}(M_Z^2)}{M_Z^2} - \frac{\Pi_{WW,\rm SM}(M_W^2)}{M_W^2}\right]. \end{aligned} \tag{24}$$

2. *Effective mixing angle definition of* $\sin^2\theta_{\rm eff}$

One could take as input parameters, G_μ, α, and the effective weak mixing angle, $\sin\theta_{\rm eff} \equiv s_{\theta,\rm eff}$. The effective weak mixing angle is defined in terms of the electron coupling to the Z:

$$L = \frac{e}{2\cos\theta_{\rm eff}\sin\theta_{\rm eff}}\bar{e}\gamma_\mu(v_e - a_e\gamma_5)eZ^\mu \tag{25}$$

where,

$$v_e = -\frac{1}{2} + 2\sin^2\theta_{\rm eff} \qquad a_e = -\frac{1}{2}. \tag{26}$$

In this scheme,

$$\frac{\delta s_{\theta,\rm eff}^2}{s_{\theta,\rm eff}^2} = \left(\frac{c_{\theta,\rm eff}}{s_{\theta,\rm eff}}\right)\frac{\Pi_{\gamma Z,\rm SM}(M_Z^2)}{M_Z^2} + \mathcal{O}(m_e^2). \tag{27}$$

This scheme is useful for comparing with the predictions of the triplet model using the renormalization scheme of Refs. [4,5].

3. *"M_Z" Definition of* $\sin\theta_Z$

A third scheme for renormalizing the SM takes as inputs $\alpha(M_Z)$, G_μ, and M_Z and defines $\sin\theta_Z \equiv s_Z$, $\cos\theta_Z \equiv c_Z$ in terms of,

$$\sin(2\theta_Z) \equiv \sqrt{\frac{4\pi\alpha(M_Z)}{\sqrt{2}G_\mu M_Z^2}}, \tag{28}$$

where

$$\begin{aligned} \frac{\delta s_Z^2}{s_Z^2} &= \frac{c_Z^2}{c_Z^2 - s_Z^2}\left(\frac{\Pi_{\gamma\gamma,\rm SM}(M_Z^2)}{M_Z^2} + \frac{2s_Z}{c_Z}\frac{\Pi_{\gamma Z,\rm SM}(0)}{M_Z^2}\right. \\ &\quad \left. - \frac{\Pi_{ZZ,\rm SM}(M_Z^2)}{M_Z^2} + \frac{\Pi_{WW,\rm SM}(0)}{M_W^2}\right). \end{aligned} \tag{29}$$

The s_Z scheme is useful for comparing with the predictions of the triplet model using the renormalization scheme advocated in Ref. [19].

B. $Y = 0$ Triplet

In this section, we consider the one-loop renormalization of the triplet model. We are particularly interested in the approach of the triplet model to the SM in different limits and in the scheme dependence of our results. Since $\rho \neq 1$ at tree level in the triplet model, four input parameters (along with the Higgs mass) are required for the electroweak renormalization [1,5,6,14]. We will consider

[2]Equation (20) implicitely defines our sign conventions for Π_{XY}. We decompose the two-point functions as $\Pi_{XY}^{\mu\nu}(k^2) = g^{\mu\nu}\Pi_{XY}(k^2) + k^\mu k^\nu B_{XY}(k^2)$ and label the SM contributions as $\Pi_{XY,\rm SM}$.

two possible renormalization schemes. The first scheme uses four measured low-energy parameters as inputs, while the second employs three low-energy parameters plus a running triplet VEV, $v'(\mu)$:

(i) *Scheme 1*: Input α, M_Z, G_μ and $\sin^2\theta_{\text{eff}}$

(ii) *Scheme 2*: Input α, M_Z, G_μ and $v'(\mu)$.

In both schemes, the W boson mass is a predicted quantity. Below we discuss the dependence of the prediction for the W mass on the renormalization scheme and focus on the approach to the SM limit as the triplet VEV becomes small, $v' \to 0$, or alternatively as M_{K^0} and $M_{H^+} \to \infty$.

1. Triplet model, Scheme 1

The renormalization of the triplet model in Scheme 1 has been discussed in Refs. [3–5]. The input parameters, α, M_Z, and G_μ are given in Eq. (17), and [37]

$$\sin^2\theta_{\text{eff}} = .2324 \pm .0012. \tag{30}$$

The relation,

$$\rho = \frac{1}{c_\delta^2} = \frac{M_W^2}{M_Z^2 c_{\theta,\text{eff}}^2}, \tag{31}$$

implies that $\tan\delta = 2v'/v$ is not a free parameter in this scheme, but is fixed by the input parameters.

In this scheme, the W mass is given by

$$M_W^2 = \frac{\alpha\pi}{\sqrt{2} s_{\theta,\text{eff}}^2 G_\mu}(1 + \Delta r_{\text{triplet}}(\text{Scheme 1})) \tag{32}$$

and[3]

$$\Delta r_{\text{triplet}}(\text{Scheme 1}) = \frac{\Pi_{WW}(0) - \Pi_{WW}(M_W^2)}{M_W^2} + \Pi'_{\gamma\gamma}(0) + 2\frac{s_{\theta,\text{eff}}}{c_{\theta,\text{eff}}}\frac{\Pi_{\gamma Z}(0)}{M_Z^2} - \frac{\delta s_{\theta,\text{eff}}^2}{s_{\theta,\text{eff}}^2} \tag{33}$$

where

$$\frac{\delta s_{\theta,\text{eff}}^2}{s_{\theta,\text{eff}}^2} = \frac{c_{\theta,\text{eff}}}{s_{\theta,\text{eff}}}\frac{\Pi_{\gamma Z}(M_Z^2)}{M_Z^2}. \tag{34}$$

Analytic formulas for the scalar, gauge boson, and Goldstone boson contributions to the two-point functions are given in Appendix A for arbitrary values of the mixing parameters $\sin\delta$ and $\sin\gamma$. The contributions from nonzero values of $\sin\gamma$ have not appeared elsewhere.

There are three types of contributions to the two-point functions. There are contributions from the W, Z, and γ gauge bosons, the electroweak ghosts, the Goldstone bosons and the lightest neutral Higgs boson where the couplings have SM strength. These are labeled as $\Pi_{XY,\text{SM}}$ in Appendix A. It is important to remember that these are not numerically equal to the results in the SM since the relationship between the W and Z masses is different in the SM and in the triplet model. The remaining contributions, which we label $\Delta\Pi_{XY}$, are of two types. There are contributions from the SM particles with couplings proportional to $\sin\delta$ or $\sin\gamma$ which vanish for δ, $\gamma \to 0$, and there are contributions from the new particles of the triplet model, K^0 and H^+, which do not necessarily vanish for δ, $\gamma \to 0$.

Equation (33) has a form analogous to the SM results obtained using the $\sin\theta_{\text{eff}}$ scheme, $(\Delta r_{\text{SM}}^{\text{eff}})$, except that in Eq. (33) there are additional contributions to the two-point functions from K^0 and H^+, and the SM-like gauge boson, Goldstone boson, and H^0 contributions are weighted by factors of $\cos\delta$ and $\cos\gamma$. At tree level, the SM and triplet predictions for M_W are the same in this scheme. It is useful to consider the difference between Eq. (33) and the one-loop SM prediction,

$$\Delta r_{\text{triplet}}(\text{Scheme 1}) = \tilde{\Delta} r_{\text{SM}}^{\text{eff}} + \Delta_{r,1}. \tag{35}$$

The function $\tilde{\Delta} r_{\text{SM}}^{\text{eff}}$ has the same functional form as $\Delta r_{\text{SM}}^{\text{eff}}$ with the important difference that in calculating $\tilde{\Delta} r_{\text{SM}}^{\text{eff}}$, M_Z must be taken as an input in the triplet Scheme 1, while M_Z is a prediction in the $\sin\theta_{\text{eff}}$ scheme of the SM. In the limit of small mixing ($\delta \sim 0$, $\gamma \sim 0$),

$$\Delta_{r,1} \to \frac{\alpha}{\pi \sin^2\theta_{\text{eff}}}\left[\frac{F_{22}(M_W^2, M_{K^0}, M_{H^+})}{M_W^2} - \frac{F_{22}(M_Z^2, M_{H^+}, M_{H^+})}{M_Z^2}\right] \tag{36}$$

where

$$F_{22}(k^2, m_1, m_2) = B_{22}(k^2, m_1, m_2) - B_{22}(0, m_1, m_2). \tag{37}$$

The small mixing limit further simplifies in the limit that $M_{K^0}, M_{H^+} \gg M_W, M_Z$ and $|M_{K^0}^2 - M_{H^+}^2| \ll M_{K^0}^2$

$$\Delta_{r,1} \to \frac{\alpha}{24\pi\sin^2\theta_{\text{eff}}}\left\{\frac{M_{K^0}^2 - M_{H^+}^2}{M_{H^+}^2}\right\} + \ldots. \tag{38}$$

Equation (38) is independent of the light Higgs boson mass and can be either positive or negative depending on the sign of $M_{K^0} - M_{H^+}$.

In Fig. 3, we show the approach of the triplet model to the one-loop SM prediction (in the $\sin^2\theta_{\text{eff}}$ renormalization scheme) as M_{H^+} becomes large. The SM prediction for M_W is calculated using Eqs. (22) and (27), while the triplet prediction for M_W is calculated using Eqs. (33) and (34). For small mixing, and $M_{K^0} = M_{H^+}$, the one-loop prediction for M_W in the triplet model differs negligibly from the SM prediction. As the mass splitting, $|M_{K^0} - M_{H^+}|$ is increased, significant differences from the SM prediction are seen at small M_{H^+}. The remainder term, $\Delta_{r,1}$, never

[3]We neglect the finite contribution from vertex and box diagrams, although the pole contributions are included in order to make our result finite and gauge invariant. The vertex and box corrections in the triplet model can be found in Ref. [5].

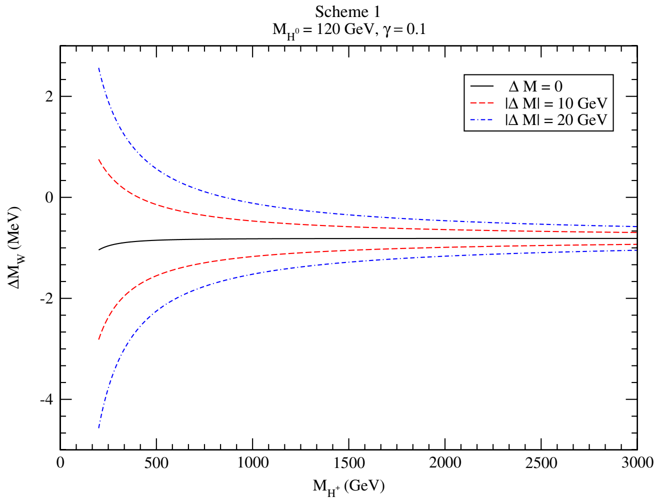

FIG. 3 (color online). Difference between the one-loop corrected values M_W(Triplet, Scheme 1) and M_W(SM, $\sin\theta_{\rm eff}$ Scheme) as a function of the charged Higgs mass, M_{H^+}, for small mixing in the neutral sector, $\gamma = 0.1$ (which corresponds to $v' \sim 6.8$ GeV). The mass difference between the scalars is $\Delta M = M_{H^+} - M_{K^0}$.

goes exactly to zero, because the triplet model has M_Z as an input, while the SM computes M_Z in the $\sin\theta_{\rm eff}$ scheme. We recall from Sec. II that in the limit $M_{K^0} = M_{H^+}$, the only consistent solution to the minimization of the potential is $v' = 0$ and $c_\delta = c_\gamma = 1$. In this limit, $\rho_0 = 1$ and the only difference between the prediction of triplet model and the SM arises from the different input values of M_Z.

2. Triplet model, Scheme 2

In Scheme 2, the input parameters are α, M_Z, G_μ and a running $v'(\mu)$. This scheme has been advocated in Ref. [19] as being more natural than Scheme 1, in that it has three measured input parameters as does the SM, while v' is unknown. We will treat v' as a running $\overline{\rm MS}$ parameter. Of particular interest is the $v' \to 0$ limit and the approach to the SM as M_{K^0} and $M_{H^+} \to \infty$.

As usual, the W boson mass is defined by,

$$M_W^2 = \frac{\alpha\pi}{\sqrt{2}s_\theta^2 G_\mu}(1 + \Delta r_{\rm triplet}(\text{Scheme 2})) \qquad (39)$$

where[4]

$$\Delta r_{\rm triplet}(\text{Scheme 2}) = \frac{\Pi_{WW}(0) - \Pi_{WW}(M_W^2)}{M_W^2} + \frac{\Pi_{\gamma\gamma}(M_Z^2)}{M_Z^2} + \frac{2\hat{s}_Z}{\hat{c}_Z}\frac{\Pi_{\gamma Z}(0)}{M_Z^2} - \frac{\delta\hat{s}_Z^2}{\hat{s}_Z^2}. \qquad (40)$$

[4]Again, we neglect the small finite contributions from the vertex and box diagrams, although the pole contributions are included in order to make our result finite and gauge independent.

At tree level,

$$G_{\mu 0} = \frac{1}{\sqrt{2}(v_0^2 + 4v_0'^2)}, \qquad (41)$$

where v_0 and v_0' are the tree-level VEVs. Using

$$M_{Z_0}^2 = \frac{e_0^2}{4\hat{s}_{Z0}^2\hat{c}_{Z0}^2} v_0^2 \qquad (42)$$

and Eq. (41), we find the weak mixing angle,

$$\hat{s}_{Z0}^2\hat{c}_{Z0}^2 = \frac{\pi\alpha_0 v_0^2}{M_{Z_0}^2} = \frac{\pi\alpha_0}{M_{Z_0}^2}\left[\frac{1}{\sqrt{2}G_{\mu 0}} - 4v_0'^2\right]. \qquad (43)$$

This scheme is similar to the M_Z scheme for the SM described in Eq. (28) in the limit $v_0' \to 0$. At tree level $\hat{s}_{Z0}$ is defined in terms of the input parameters as

$$\hat{s}_{Z0}^2 = \frac{1}{2}\left(1 - \sqrt{1 - \frac{4\pi\alpha_0}{\sqrt{2}M_{Z_0}^2 G_{\mu 0}}(1 - 4\sqrt{2}G_{\mu 0}v_0'^2)}\right), \qquad (44)$$

and the one-loop corrected value for the mixing angle is

$$\frac{\delta\hat{s}_Z^2}{\hat{s}_Z^2} = \frac{\hat{c}_Z^2}{\hat{c}_Z^2 - \hat{s}_Z^2}\left\{\Pi'_{\gamma\gamma}(0) + \frac{2\hat{s}_Z}{\hat{c}_Z}\frac{\Pi_{\gamma Z}(0)}{M_Z^2} - \frac{\Pi_{ZZ}(M_Z^2)}{M_Z^2} + \frac{1}{1 - 4\sqrt{2}v'^2 G_\mu}\left[\frac{\Pi_{WW}(0)}{M_W^2} - 4\sqrt{2}G_\mu v'^2\frac{\delta v'^2}{v'^2}\right]\right\}. \qquad (45)$$

Finally, we need to define the renormalized triplet VEV:

$$v_0'^2 = v'^2\left(1 + \frac{\delta v'^2}{v'^2}\right). \qquad (46)$$

There is no compelling physical definition for the v' counterterm and we simply utilize an $\overline{\rm MS}$ definition and retain only the poles necessary to cancel the divergences.

In Fig. 4, we compare the one-loop corrected prediction for M_W in the M_Z scheme of the SM, with the one-loop corrected value for M_W in the triplet model, Scheme 2, with $\gamma = 0$ and $v' = 0$. For $\gamma = 0$ and $v' = 0$, the only consistent solution to the minimization of the potential is $M_{H^+} = M_{K^0}$ and for these parameters, the contribution of the triplet model quickly decouples as M_{H^+} becomes large and the SM result is exactly recovered.

The situation is quite different for nonzero v' as shown in Figs. 5 and 6. The large effects can be understood from Eq. (45),

$$\frac{\delta\hat{s}_Z^2}{\hat{s}_Z^2} \sim \frac{\hat{c}_Z^2}{\hat{c}_Z^2 - \hat{s}_Z^2}\left\{-\frac{\Pi_{ZZ}(M_Z^2)}{M_Z^2} + \frac{1}{1 - 4\sqrt{2}v'^2 G_\mu}\frac{\Pi_{WW}(0)}{M_W^2}\right\}. \qquad (47)$$

Both $\frac{\Pi_{ZZ}(M_Z^2)}{M_Z^2}$ and $\frac{\Pi_{WW}(0)}{M_W^2}$ have contributions which grow

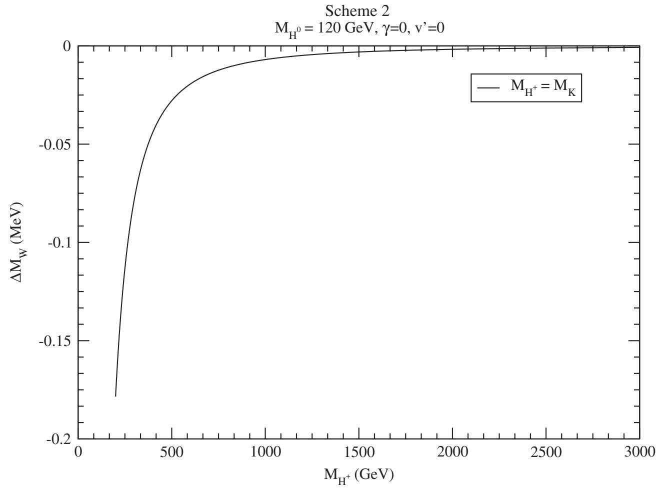

FIG. 4. Difference between the one-loop corrected values M_W(Triplet, Scheme 2) and M_W(SM, M_Z Scheme) as a function of the charged Higgs mass, M_{H^+}, for zero mixing in the neutral sector ($\gamma = 0$) and for $v' = 0$.

with $M^2_{H^+}$ and $M^2_{K^0}$ which cancel in Eq. (47) when $v' = 0$. The cancellation is spoiled for nonzero v' leading to the large effects observed in Figs. 5 and 6. Figures 5 and 6 show a modest sensitivity of our results to nonzero mixing in the neutral sector ($\gamma \neq 0$).

Equation (47) makes it apparent that tadpole diagrams (shown in Fig. 7) do not cancel for nonzero v' and make a contribution,

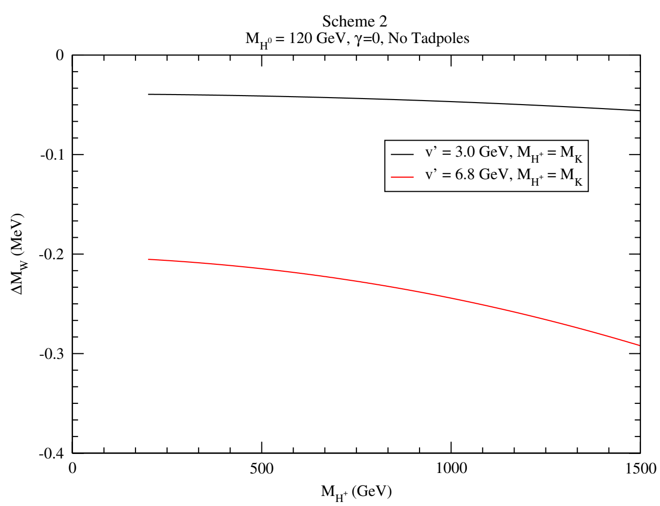

FIG. 5 (color online). Difference between the one-loop corrected values M_W(Triplet, Scheme 2) and M_W(SM, M_Z Scheme) as a function of the charged Higgs mass, M_{H^+}, for no mixing in the neutral sector ($\gamma = 0.0$) and for $v' = 3$ GeV and $v' = 6.8$ GeV. Tadpoles are not included in this plot.

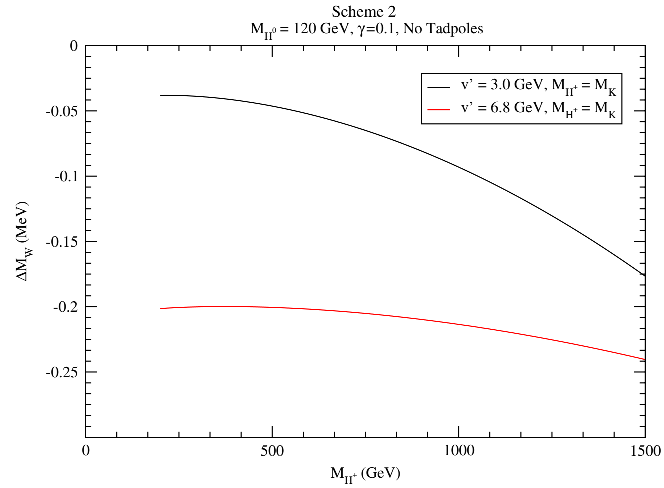

FIG. 6 (color online). Difference between the one-loop corrected values M_W(Triplet, Scheme 2) and M_W(SM, M_Z Scheme) as a function of the charged Higgs mass, M_{H^+}, for small mixing in the neutral sector ($\gamma = 0.1$) and for $v' = 3$ GeV and $v' = 6.8$ GeV. Tadpoles are not included in this plot.

$$\Delta r_{\rm triplet}(\text{Scheme 2})^{\rm tadpole} = -\frac{\hat{c}_Z^2}{\hat{c}_Z^2 - \hat{s}_Z^2}\left\{-\frac{\Pi_{ZZ}^{\rm tadpole}}{M_Z^2} + \frac{1}{1 - 4\sqrt{2}v'^2 G_\mu}\frac{\Pi_{WW}^{\rm tadpole}}{M_W^2}\right\}, \tag{48}$$

where the tadpole contributions are

$$\begin{aligned}\Pi_{WW}^{\rm tadpole} &= -gM_W\left\{(c_\delta c_\gamma + 2s_\delta s_\gamma)\frac{\mathcal{T}_{\mathcal{H}}}{M^2_{H^0}} + (-c_\delta s_\gamma + 2s_\delta c_\gamma)\frac{\mathcal{T}_{\mathcal{K}}}{M^2_{K^0}}\right\}\\ \Pi_{ZZ}^{\rm tadpole} &= -g\frac{M_Z}{\hat{c}_Z}\left\{c_\gamma\frac{\mathcal{T}_{\mathcal{H}}}{M^2_{H^0}} - s_\gamma\frac{\mathcal{T}_{\mathcal{K}}}{M^2_{K^0}}\right\}.\end{aligned} \tag{49}$$

The scalar self-couplings are given in Appendix C [20] and lead to

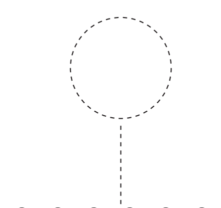

FIG. 7. Tadpole contribution to the gauge boson two-point function.

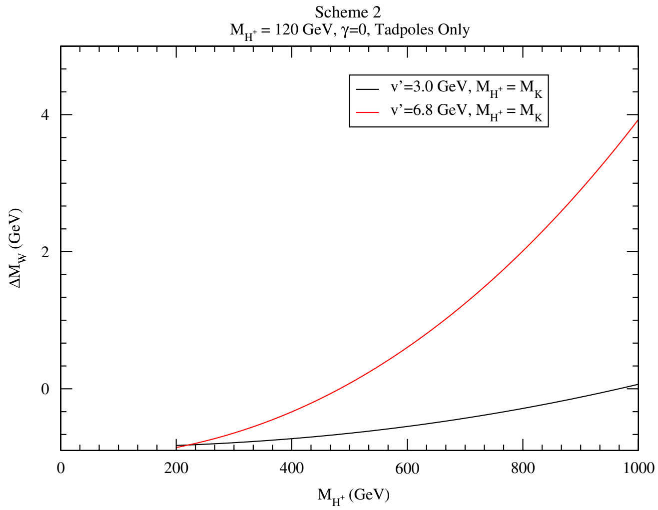

FIG. 8 (color online). Difference between the tadpole contribution to M_W in Scheme 2 and the one-loop prediction for M_W(SM, M_Z Scheme) as a function of the charged Higgs mass, M_{H^+} for zero mixing in the neutral sector ($\gamma = 0.0$) and for $v' = 5$ GeV and $v' = 9$ GeV.

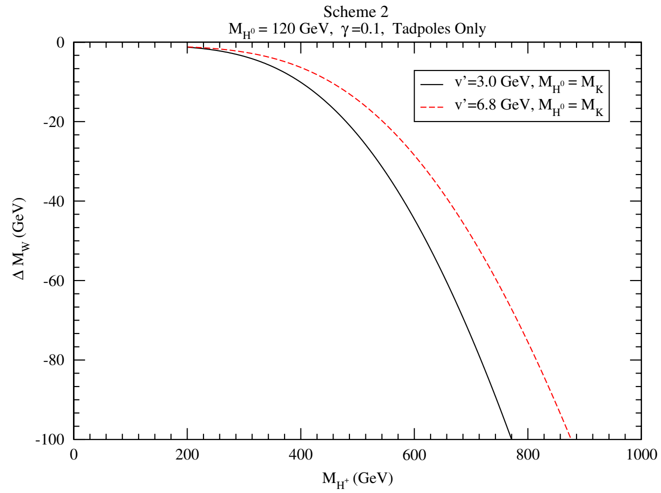

FIG. 9 (color online). Difference between the tadpole contribution to M_W in Scheme 2 and the one-loop prediction for M_W(SM, M_Z Scheme) as a function of the charged Higgs mass, M_{H^+} for small mixing in the neutral sector ($\gamma = 0.1$) and for $v' = 5$ GeV and $v' = 9$ GeV.

$$\begin{aligned}\mathcal{T}_H &= -\frac{1}{16\pi^2}\bigg\{\frac{g_{HHH}}{2}A_0(M_{H^0}) + \frac{g_{HKK}}{2}A_0(M_{K^0}) + \frac{g_{HG^0G^0}}{2}A_0(M_Z) + g_{HG^+G^-}A_0(M_W) + g_{H^0H^+H^-}A_0(M_{H^+}) \\ &\quad - gM_W(c_\delta c_\gamma + 2s_\delta s_\gamma)(4-2\epsilon)A_0(M_W) - gM_Z\frac{c_\gamma}{c_\theta}(4-2\epsilon)A_0(M_Z)\bigg\} \\ \mathcal{T}_K &= -\frac{1}{16\pi^2}\bigg\{\frac{g_{KHH}}{2}A_0(M_{H^0}) + \frac{g_{KKK}}{2}A_0(M_{K^0}) + \frac{g_{KG^0G^0}}{2}A_0(M_Z) + g_{KG^+G^-}A_0(M_W) + g_{K^0H^+H^-}A_0(M_{H^+}) \\ &\quad - gM_W(-c_\delta s_\gamma + 2s_\delta c_\gamma)(4-2\epsilon)A_0(M_W) + gM_Z\frac{s_\gamma}{c_\theta}(4-2\epsilon)A_0(M_Z)\bigg\}.\end{aligned} \tag{50}$$

The tadpole diagrams generate terms which grow with mass-squared, and the contribution of the tadpole diagrams in Scheme 2 to M_W is shown in Figs. 8 and 9. The large size of the tadpole contributions makes it clear that $\delta v'$ must be defined in such a manner as to cancel the contributions from the tadpole diagrams in order to have a sensible theory. The tadpole contributions grow with v'^2 as expected and have a large dependence on γ.

V. DECOUPLING AND CONCLUSIONS

We have considered the simplest possible model with $\rho \neq 1$ at tree level: a model with a real scalar $SU(2)$ triplet in addition to the SM Higgs doublet and have presented results for the one-loop prediction for the W mass in two different renormalization schemes. Our results are shown as differences from the SM predictions. A correct renormalization scheme in the triplet model requires four input parameters, in contrast to the three required in the electroweak sector of the SM.

In the first scheme, four low-energy measured parameters are used as inputs and the theory is renormalized as a low-energy theory. The effects of the scalar loops are negligible for large triplet scalar masses, when the mass difference between the scalar masses associated with the triplets is small ($|M_{K^0} - M_{H^+}| \ll M_{K^0}$). This renormalization scheme fixes the triplet v' in terms of the input parameters and so the limit $v' \to 0$ cannot be taken. In the second scheme, three low-energy parameters and a running triplet VEV are used as inputs. The nonzero triplet VEV generates large contributions from tadpole diagrams which must be cancelled by hand by an appropriate definition of the triplet VEV renormalization condition. This fine-tuning implies a lack of predictivity for the model. Neither renormalization scheme is entirely satisfactory, although our results clearly demonstrate the importance of scalar loops in theories with $\rho \neq 1$ at tree level.

ACKNOWLEDGMENTS

The work of S. D. (C. J.) is supported by the U.S. Department of Energy under Grant No. DE-AC02-98CH10886 (DE-AC02-06CH11357). The work of M.-C. C. is supported, in part, by the National Science

Foundation under Grant No. PHY-0709742. S. D. thanks the SLAC theory group for their hospitality, where this work was begun.

APPENDIX A: 2-POINT CONTRIBUTIONS

In general, we write

$$\Pi_{XY}(k^2) = \Pi_{XY,\mathrm{SM}}(k^2) + \Delta\Pi_{XY}(k^2). \qquad \text{(A1)}$$

The contributions labeled $\Pi_{XY,\mathrm{SM}}$ have the same functional form as the SM contributions from gauge and Goldstone bosons, ghosts, and the lightest neutral Higgs, H^0, in the $\rho_0 = 1$ limit. We remind the reader yet again that the $\Pi_{XY,\mathrm{SM}}$ terms utilize different relations between M_Z and M_W in the triplet and SM and hence are not in general numerically equal. The remainder, $\Delta\Pi_{XY}$, contains terms which vanish in the limit $\sin\delta$, $\sin\gamma \to 0$, and also the contributions of K^0 and H^+, which need not vanish in the $\sin\delta = \sin\gamma = 0$ limit. The SM-like contributions agree with those found in Ref. [34] and the triplet contributions for $\sin\gamma = 0$ agree with Ref. [5]. The contributions for nonzero γ are new.

From Fig. 10, the standard model-like contributions in Feynman gauge are

$$\begin{aligned}
\Pi^1_{WW,\mathrm{SM}}(k^2) &= \frac{\alpha}{16\pi s_\theta^2}\{A_0(M_{H^0}) + A_0(M_Z) + 2A_0(M_W)\} \\
\Pi^1_{ZZ,\mathrm{SM}}(k^2) &= \frac{\alpha}{16\pi s_\theta^2 c_\theta^2}\{A_0(M_{H^0}) + A_0(M_Z) \\
&\quad + 2(c_\theta^2 - s_\theta^2)^2 A_0(M_W)\} \\
\Pi^1_{\gamma\gamma,\mathrm{SM}}(k^2) &= \frac{\alpha}{2\pi}[A_0(M_W)] \\
\Pi^1_{\gamma Z,\mathrm{SM}}(k^2) &= \frac{\alpha}{4\pi s_\theta c_\theta}[(s_\theta^2 - c_\theta^2)A_0(M_W)].
\end{aligned} \qquad \text{(A2)}$$

The non-standard model contributions from Fig. 10 are

$$\begin{aligned}
\Delta\Pi^1_{WW}(k^2) &= \frac{\alpha}{16\pi s_\theta^2}\{-3s_\gamma^2[A_0(M_{K^0}) - A_0(M_{H^0})] + 2s_\delta^2[A_0(M_W) - A_0(M_{H^+})] + 4[A_0(M_{K^0}) + A_0(M_{H^+})]\} \\
\Delta\Pi^1_{ZZ}(k^2) &= \frac{\alpha}{16\pi s_\theta^2 c_\theta^2}\{s_\gamma^2[A_0(M_{K^0}) - A_0(M_{H^0})] + 2s_\delta^2(1 - 4c_\theta^2)[A_0(M_{H^+}) - A_0(M_W)] + 8c_\theta^4 A_0(M_{H^+})\} \\
\Delta\Pi^1_{\gamma\gamma}(k^2) &= \frac{\alpha}{2\pi}A_0(M_{H^\pm}) \qquad \Delta\Pi^1_{\gamma Z}(k^2) = \frac{\alpha}{4\pi s_\theta c_\theta}\{s_\delta^2[A_0(M_{H^+}) - A_0(M_W)] - 2c_\theta^2 A_0(M_{H^+})\}.
\end{aligned} \qquad \text{(A3)}$$

From Fig. 11, the SM-like contributions are

$$\begin{aligned}
\Pi^2_{WW,\mathrm{SM}}(k^2) &= \frac{\alpha}{4\pi}\frac{M_W^2}{s_\theta^2}\left\{\frac{s_\theta^4}{c_\theta^2}B_0(k^2, M_Z, M_W) + s_\theta^2 B_0(k^2, 0, M_W) + B_0(k^2, M_{H^0}, M_W)]\right\} \\
\Pi^2_{ZZ,\mathrm{SM}}(k^2) &= \frac{\alpha}{4\pi}\frac{M_Z^2}{s_\theta^2}\left\{\frac{1}{c_\theta^2}B_0(k^2, M_{H^0}, M_Z) + 2s_\theta^4 B_0(k^2, M_W, M_W)\right\} \\
\Pi^2_{\gamma\gamma,\mathrm{SM}}(k^2) &= \frac{\alpha}{2\pi}M_W^2 B_0(k^2, M_W, M_W) \qquad \Pi^2_{\gamma Z,\mathrm{SM}}(k^2) = \frac{\alpha}{2\pi}M_W^2\frac{s_\theta}{c_\theta}B_0(k^2, M_W, M_W).
\end{aligned} \qquad \text{(A4)}$$

The non-standard model contributions from Fig. 11 are

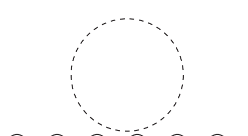

FIG. 10. Contributions from Goldstone bosons and H^0, K^0 and H^+ to the gauge boson two-point functions.

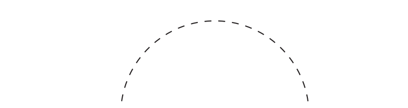

FIG. 11. Contribution to the gauge boson two-point function with one internal scalar and one internal vector boson.

$$\begin{aligned}
\Delta\Pi^2_{WW}(k^2) &= \frac{\alpha}{4\pi}\frac{M_W^2}{s_\theta^2}\bigg\{\frac{c_\delta^2 s_\delta^2}{c_\theta^2}[B_0(k^2, M_Z, M_{H^+}) - B_0(k^2, M_Z, M_W)] + (4s_\delta c_\delta s_\gamma c_\gamma - s_\gamma^2 + 5s_\delta^2 s_\gamma^2)[B_0(k^2, M_{H^0}, M_W) \\
&\quad - B_0(k^2, M_{K^0}, M_W)] + s_\delta^2\bigg[\frac{c_\theta^2 - s_\theta^2}{c_\theta^2}B_0(k^2, M_Z, M_W) - B_0(k^2, M_{H^0}, M_W) + 4B_0(k^2, M_{K^0}, M_W)\bigg]\bigg\} \\
\Delta\Pi^2_{ZZ}(k^2) &= \frac{\alpha}{4\pi}\frac{M_Z^2}{s_\theta^2}\bigg\{\frac{s_\gamma^2}{c_\theta^2}[B_0(k^2, M_{K^0}, M_Z) - B_0(k^2, M_{H^0}, M_Z)] + 2s_\delta^2[B_0(k^2, M_{H^+}, M_W) - B_0(k^2, M_W, M_W)] \\
&\quad + 2\frac{s_\delta^2}{c_\delta^2}c_\theta^4 B_0(k^2, M_W, M_W)\bigg\} \\
\Delta\Pi^2_{\gamma\gamma}(k^2) &= 0 \qquad \Delta\Pi^2_{\gamma Z}(k^2) = -\frac{\alpha}{2\pi}M_W^2\frac{s_\delta^2}{s_\theta c_\theta}B_0(k^2, M_W, M_W).
\end{aligned} \tag{A5}$$

From Fig. 12, the SM-like contributions are

$$\begin{aligned}
\Pi^3_{WW,\mathrm{SM}}(k^2) &= -\frac{\alpha}{4\pi s_\theta^2}\{B_{22}(k^2, M_{H^0}, M_W) + B_{22}(k^2, M_Z, M_W)\} \\
\Pi^3_{ZZ,\mathrm{SM}}(k^2) &= -\frac{\alpha}{4\pi s_\theta^2 c_\theta^2}\{B_{22}(k^2, M_{H^0}, M_Z) + (c_\theta^2 - s_\theta^2)^2 B_{22}(k^2, M_W, M_W)\} \\
\Pi^3_{\gamma\gamma,\mathrm{SM}}(k^2) &= -\frac{\alpha}{\pi}B_{22}(k^2, M_W, M_W) \qquad \Pi^3_{\gamma Z,\mathrm{SM}}(k^2) = \frac{\alpha}{2\pi c_\theta s_\theta}(c_\theta^2 - s_\theta^2)B_{22}(k^2, M_W, M_W).
\end{aligned} \tag{A6}$$

From Fig. 12, the non-SM contributions are

$$\begin{aligned}
\Delta\Pi^3_{WW}(k^2) &= -\frac{\alpha}{4\pi s_\theta^2}\{4s_\gamma c_\gamma s_\delta c_\delta(B_{22}(k^2, M_{K^0}, M_{H^+}) - B_{22}(k^2, M_{H^0}, M_{H^+}) + B_{22}(k^2, M_{H^0}, M_W) - B_{22}(k^2, M_{K^0}, M_W)) \\
&\quad + 4s_\gamma^2 s_\delta^2(B_{22}(k^2, M_{H^0}, M_W) - B_{22}(k^2, M_{H^0}, M_{H^+})) + s_\gamma^2 s_\delta^2(B_{22}(k^2, M_{K^0}, M_{H^+}) - B_{22}(k^2, M_{H^0}, M_{H^+})) \\
&\quad + 4c_\gamma^2 s_\delta^2(B_{22}(k^2, M_{K^0}, M_W) - B_{22}(k^2, M_{K^0}, M_{H^+})) + s_\gamma^2 c_\delta^2(B_{22}(k^2, M_{K^0}, M_W) - B_{22}(k^2, M_{H^0}, M_W)) \\
&\quad + s_\delta^2(B_{22}(k^2, M_Z, M_{H^+}) - B_{22}(k^2, M_Z, M_W) + B_{22}(k^2, M_{H^0}, M_{H^+}) - B_{22}(k^2, M_{H^0}, M_W)) \\
&\quad + 4s_\gamma^2(B_{22}(k^2, M_{H^0}, M_{H^+}) - B_{22}(k^2, M_{K^0}, M_{H^+})) + 4B_{22}(k^2, M_{K^0}, M_{H^+})\} \\
\Delta\Pi^3_{ZZ}(k^2) &= -\frac{\alpha}{4\pi s_\theta^2 c_\theta^2}\{s_\gamma^2[B_{22}(k^2, M_{K^0}, M_Z) - B_{22}(k^2, M_{H^0}, M_Z)] + s_\delta^2[4c_\theta^2(B_{22}(k^2, M_W, M_W) - B_{22}(k^2, M_{H^+}, M_{H^+})) \\
&\quad + s_\delta^2(B_{22}(k^2, M_{H^+}, M_{H^+}) - B_{22}(k^2, M_{H^+}, M_W) + B_{22}(k^2, M_W, M_W) - B_{22}(k^2, M_{H^+}, M_W)) \\
&\quad + 2(B_{22}(k^2, M_{H^+}, M_W) - B_{22}(k^2, M_W, M_W))] + 4c_\theta^4 B_{22}(k^2, M_{H^+}, M_{H^+})\} \\
\Delta\Pi^3_{\gamma\gamma}(k^2) &= -\frac{\alpha}{\pi}B_{22}(k^2, M_{H^+}, M_{H^+}) \\
\Delta\Pi^3_{\gamma Z}(k^2) &= \frac{\alpha}{2\pi c_\theta s_\theta}\{s_\delta^2[B_{22}(k^2, M_W, M_W) - B_{22}(k^2, M_{H^+}, M_{H^+})] + 2c_\theta^2 B_{22}(k^2, M_{H^+}, M_{H^+})\}.
\end{aligned} \tag{A7}$$

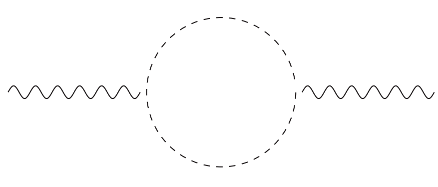

FIG. 12. Contribution to the gauge boson two-point function from Goldstone boson and scalar loops.

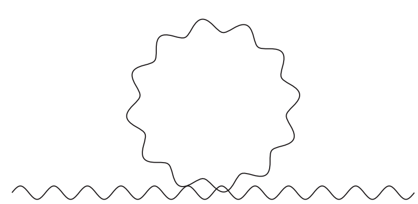

FIG. 13. Contribution to gauge boson two-point function from SM gauge bosons in loop.

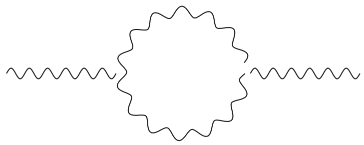

FIG. 14. Contribution to the gauge boson two-point function from SM gauge bosons in loop.

There are additional contributions which only contribute to $\Pi_{\rm SM}$, which we list for completeness [34]. From Fig. 13,

$$\begin{aligned}
\Pi^4_{WW,{\rm SM}}(k^2) &= \frac{\alpha}{4\pi s_\theta^2}(3-2\epsilon)[A_0(M_W)+c_\theta^2 A_0(M_Z)] \\
\Pi^4_{ZZ,{\rm SM}}(k^2) &= \frac{\alpha c_\theta^2}{2\pi s_\theta^2}(3-2\epsilon)A_0(M_W) \\
\Pi^4_{\gamma\gamma,{\rm SM}}(k^2) &= \frac{\alpha}{2\pi}(3-2\epsilon)A_0(M_W) \\
\Pi^4_{\gamma Z,{\rm SM}}(k^2) &= -\frac{\alpha c_\theta}{2\pi s_\theta}(3-2\epsilon)A_0(M_W).
\end{aligned} \tag{A8}$$

From Fig. 14,

$$\begin{aligned}
\Pi^5_{WW,{\rm SM}}(k^2) &= \frac{\alpha}{4\pi s_\theta^2}[s_\theta^2 A_1(k^2,0,M_W) \\
&\quad + c_\theta^2 A_1(k^2,M_Z,M_W)] \\
\Pi^5_{ZZ,{\rm SM}}(k^2) &= \frac{\alpha c_\theta^2}{4\pi s_\theta^2}A_1(k^2,M_W,M_W) \\
\Pi^5_{\gamma\gamma,{\rm SM}}(k^2) &= \frac{\alpha}{4\pi}A_1(k^2,M_W,M_W) \\
\Pi^5_{\gamma Z,{\rm SM}}(k^2) &= -\frac{\alpha c_\theta}{4\pi s_\theta}A_1(k^2,M_W,M_W),
\end{aligned} \tag{A9}$$

where,

$$\begin{aligned}
A_1(k^2,m_1,m_2) &= -A_0(m_1)-A_0(m_2) \\
&\quad -(m_1^2+m_2^2+4k^2)B_0(k^2,m_1,m_1) \\
&\quad -10B_{22}(k^2,m_1,m_2) \\
&\quad +2\left(m_1^2+m_2^2-\frac{k^2}{3}\right).
\end{aligned} \tag{A10}$$

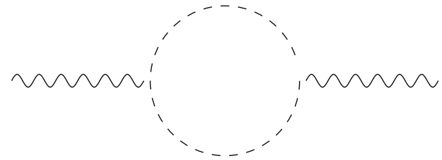

FIG. 15. Contribution to gauge boson two-point function from ghosts in loop.

From Fig. 15,

$$\begin{aligned}
\Pi^6_{WW,{\rm SM}}(k^2) &= \frac{\alpha}{2\pi s_\theta^2}[s_\theta^2 B_{22}(k^2,0,M_W) \\
&\quad + c_\theta^2 B_{22}(k^2,M_Z,M_W)] \\
\Pi^6_{ZZ,{\rm SM}}(k^2) &= \frac{\alpha c_\theta^2}{2\pi s_\theta^2}B_{22}(k^2,M_W,M_W) \\
\Pi^6_{\gamma\gamma,{\rm SM}}(k^2) &= \frac{\alpha}{2\pi}B_{22}(k^2,M_W,M_W) \\
\Pi^6_{\gamma Z,{\rm SM}}(k^2) &= -\frac{\alpha c_\theta}{2\pi s_\theta}B_{22}(k^2,M_W,M_W).
\end{aligned} \tag{A11}$$

APPENDIX B: SCALAR INTEGRALS

The scalar integrals in $n = 4 - 2\epsilon$ dimensions are defined as

$$\begin{aligned}
\frac{i}{16\pi^2}A_0(m) &= \int \frac{d^n q}{(2\pi)^n}\frac{1}{q^2-m^2} \\
\frac{i}{16\pi^2}B_0(k^2,m_1,m_2) &= \int \frac{d^n q}{(2\pi)^n} \\
&\quad \times \frac{1}{[q^2-m_1^2][(q+k)^2-m_2^2]}.
\end{aligned} \tag{B1}$$

The tensor integral is,

$$\begin{aligned}
&\frac{i}{16\pi^2}\{g^{\mu\nu}B_{22}(k^2,m_1,m_2)+k^\mu k^\nu B_{12}(k^2,m_1,m_2)\} \\
&\quad = \int \frac{d^n q}{(2\pi)^n}\frac{q^\mu q^\nu}{[q^2-m_1^2][(q+k)^2-m_2^2]}.
\end{aligned} \tag{B2}$$

APPENDIX C: SCALAR SELF-COUPLINGS

$$
\begin{aligned}
g_{HHH} &= 6\Big(vc_\gamma^3\lambda_1 + v's_\gamma^3\lambda_2 + \frac{c_\gamma s_\gamma}{2}(s_\gamma v + c_\gamma v')\lambda_3 - \frac{s_\gamma c_\gamma^2}{2}\lambda_4\Big)\\
g_{HHK} &= 2\Big(-3vs_\gamma c_\gamma^2\lambda_1 + 3s_\gamma^2 c_\gamma v'\lambda_2 + \frac{\lambda_3}{2}[-vs_\gamma(1-3c_\gamma^2) + v'c_\gamma(1-3s_\gamma^2)] - \frac{c_\gamma}{2}(1-3s_\gamma^2)\lambda_4\Big)\\
g_{HKK} &= 2\Big(3v\lambda_1 c_\gamma s_\gamma^2 + 3v'\lambda_2 c_\gamma^2 s_\gamma + \frac{\lambda_3}{2}[vc_\gamma(1-3s_\gamma^2) + v's_\gamma(1-3c_\gamma^2)] - \frac{s_\gamma}{2}(1-3c_\gamma^2)\lambda_4\Big)\\
g_{KKK} &= 6\Big(-\lambda_1 vs_\gamma^3 + \lambda_2 v'c_\gamma^3 + \frac{c_\gamma s_\gamma}{2}(-c_\gamma v + s_\gamma v')\lambda_3 - \frac{c_\gamma s_\gamma^2}{2}\lambda_4\Big)\\
g_{HG^+G^-} &= (2v\lambda_1 c_\gamma c_\delta^2 + 2v'\lambda_2 s_\gamma s_\delta^2 + \lambda_3(vc_\gamma s_\delta^2 + v's_\gamma c_\delta^2) + c_\delta\lambda_4(2c_\gamma s_\delta + s_\gamma c_\delta))\\
g_{HH^+H^-} &= (2v\lambda_1 c_\gamma s_\delta^2 + 2v'\lambda_2 s_\gamma c_\delta^2 + \lambda_3(vc_\gamma c_\delta^2 + v's_\gamma s_\delta^2) - s_\delta\lambda_4(2c_\gamma c_\delta - s_\gamma s_\delta))\\
g_{KG^+G^-} &= (-2v\lambda_1 s_\gamma c_\delta^2 + 2v'\lambda_2 c_\gamma s_\delta^2 + \lambda_3(-vs_\gamma s_\delta^2 + v'c_\gamma c_\delta^2) + c_\delta\lambda_4(-2s_\gamma s_\delta + c_\gamma c_\delta))\\
g_{KH^+H^-} &= (-2v\lambda_1 s_\gamma s_\delta^2 + 2v'\lambda_2 c_\gamma c_\delta^2 + \lambda_3(-vs_\gamma c_\delta^2 + v'c_\gamma s_\delta^2) + s_\delta\lambda_4(2s_\gamma c_\delta + c_\gamma s_\delta))\\
g_{HG^0G^0} &= \Big(\lambda_1 c_\gamma v + \frac{\lambda_3}{2}v's_\gamma - \frac{\lambda_4}{2}c_\gamma\Big)\\
g_{KG^0G^0} &= \Big(-\lambda_1 s_\gamma v + \frac{\lambda_3}{2}v'c_\gamma + \frac{\lambda_4}{2}s_\gamma\Big)
\end{aligned}
\tag{C1}
$$

[1] J. Erler and P. Langacker, arXiv:hep-ph/0407097.
[2] J. Erler and P. Langacker, arXiv:0807.3023.
[3] M.-C. Chen, S. Dawson, and T. Krupovnickas, Phys. Rev. D **74**, 035001 (2006).
[4] M.-C. Chen, S. Dawson, and T. Krupovnickas, Int. J. Mod. Phys. A **21**, 4045 (2006).
[5] T. Blank and W. Hollik, Nucl. Phys. **B514**, 113 (1998).
[6] B. W. Lynn and E. Nardi, Nucl. Phys. **B381**, 467 (1992).
[7] N. Arkani-Hamed, A. G. Cohen, and H. Georgi, Phys. Lett. B **513**, 232 (2001).
[8] N. Arkani-Hamed, A. G. Cohen, E. Katz, and A. E. Nelson, J. High Energy Phys. 07 (2002) 034.
[9] N. Arkani-Hamed *et al.*, J. High Energy Phys. 08 (2002) 021.
[10] S. Chang and J. G. Wacker, Phys. Rev. D **69**, 035002 (2004).
[11] W. Skiba and J. Terning, Phys. Rev. D **68**, 075001 (2003).
[12] S. Chang, J. High Energy Phys. 12 (2003) 057.
[13] M. Schmaltz and D. Tucker-Smith, Annu. Rev. Nucl. Part. Sci. **55**, 229 (2005).
[14] M.-C. Chen, Mod. Phys. Lett. A **21**, 621 (2006).
[15] G. Passarino, Nucl. Phys. **B361**, 351 (1991).
[16] G. Passarino, Phys. Lett. B **247**, 587 (1990).
[17] M. Czakon, J. Gluza, F. Jegerlehner, and M. Zralek, Eur. Phys. J. C **13**, 275 (2000).
[18] M. Czakon, M. Zralek, and J. Gluza, Nucl. Phys. **B573**, 57 (2000).
[19] P. H. Chankowski, S. Pokorski, and J. Wagner, Eur. Phys. J. C **50**, 919 (2007).
[20] P. H. Chankowski and J. Wagner, Phys. Rev. D **77**, 025033 (2008).
[21] M. E. Peskin and J. D. Wells, Phys. Rev. D **64**, 093003 (2001).
[22] R. S. Chivukula, C. Hoelbling, and N. J. Evans, Phys. Rev. Lett. **85**, 511 (2000).
[23] J. L. Hewett, F. J. Petriello, and T. G. Rizzo, J. High Energy Phys. 10 (2003) 062.
[24] D. Toussaint, Phys. Rev. D **18**, 1626 (1978).
[25] G. Senjanovic and A. Sokorac, Phys. Rev. D **18**, 2708 (1978).
[26] M.-C. Chen and S. Dawson, Phys. Rev. D **70**, 015003 (2004).
[27] J. R. Forshaw, D. A. Ross, and B. E. White, J. High Energy Phys. 10 (2001) 007.
[28] R. Sekhar Chivukula, N. D. Christensen, and E. H. Simmons, Phys. Rev. D **77**, 035001 (2008).
[29] T. Appelquist and J. Carazzone, Nucl. Phys. **B120**, 77 (1977).
[30] J. R. Forshaw, A. Sabio Vera, and B. E. White, J. High Energy Phys. 06 (2003) 059.
[31] A. Sirlin, Phys. Rev. D **22**, 971 (1980).
[32] A. Sirlin and W. J. Marciano, Nucl. Phys. **B189**, 442 (1981).
[33] F. Jegerlehner, "Renormalizing the Standard Model," in Proceedings of the Theoretical Advanced Study Institute in Elementary Particle Physics, (TASI), Boulder, Colo., 1990 (1991), pp. 476–590.
[34] W. Hollik, "Electroweak Radiative Corrections," in Proceedings of the 7th Summer School Jorge Andre Swieca: Particles and Fields, Sao Paulo, Brazil, 1993 (1993), pp. 169–257.
[35] C. Amsler *et al.* (Particle Data Group), Phys. Lett. B **667**, 1 (2008).
[36] M. E. Peskin and D. V. Schroeder, *An Introduction to Quantum Field Theory* (Westview Press, New York, 1995).
[37] LEP Electroweak Working Group, http://lepewwg.web.cern.ch/LEPEWWG/.